ELSEVIER

Journal of Biomechanics 35 (2002) 1581–1589

JOURNAL OF BIOMECHANICS

www.elsevier.com/locate/jbiomech
www.JBiomech.com

Extrinsic flexor muscles generate concurrent flexion of all three finger joints

Derek G. Kamper[a,b,*], T. George Hornby[a], William Z. Rymer[a,b]

[a] *Sensory Motor Performance Program, Rehabilitation Institute of Chicago, 345 E. Superior Street, Chicago, IL 606011, USA*
[b] *Department of Physical Medicine and Rehabilitation, Northwestern University, Feinberg School of Medicine, Chicago, IL, USA*

Accepted 24 June 2002

Abstract

The role of the forearm (extrinsic) finger flexor muscles in initiating rotation of the metacarpophalangeal (MCP) joint and in coordinating flexion at the MCP, the proximal interphalangeal (PIP), and distal interphalangeal (DIP) joints remains a matter of some debate. To address the biomechanical feasibility of the extrinsic flexors performing these actions, a computer simulation of the index finger was created. The model consisted of a planar open-link chain comprised of three revolute joints and four links, driven by the change in length of the flexor muscles. Passive joint characteristics, included in the model, were obtained from system identification experiments involving the application of angular perturbations to the joint of interest. Simulation results reveal that in the absence of passive joint torque, shortening of the extrinsic flexors results in PIP flexion (80°), but DIP (8°) and MCP (7°) joint extension. The inclusion of normal physiological levels of passive joint torque, however, results in simultaneous flexion of all three joints (63° for DIP, 75° for PIP, and 43° for MCP). Applicability of the simulation results was confirmed by recording finger motion produced by electrical stimulation of the extrinsic flexor muscles for the index finger. These findings support the view that the extrinsic flexor muscles can initiate MCP flexion, and produce simultaneous motion at the MCP, PIP, and DIP joints.

Keywords: Index finger; Motor control; Stiffness; Damping

1. Introduction

Proper understanding of finger biomechanics could greatly facilitate hand rehabilitation, whether through guiding reconstructive surgeries (Keith et al., 1996), neuromuscular electrical stimulation protocols (Lauer et al., 1999), or other modalities. Finger biomechanics, however, has proven difficult to comprehend, due to the seeming redundancy in muscle actuation of the joints, and to the potential for each finger muscle to affect multiple joints.

One mechanism not clearly understood is the control of flexion of the metacarpophalangeal (MCP) joints. A number of muscle tendons cross this joint on its palmar side, such as the extrinsic flexor muscles [flexor digitorum profundus (FDP) and flexor digitorum superficialis (FDS)], and the intrinsic hand muscles [the lumbricals and interossei]. As FDS and FDP do not attach to the proximal phalanx, traditionally the extrinsic flexors have been thought to have only tertiary involvement in MCP flexion, either by acting on the MCP joint only after completing flexion of the proximal interphalangeal (PIP) and distal interphalangeal (DIP) joints, respectively, or by acting only indirectly through the connection between FDP and the lumbrical (Long, 1968; Zancolli, 1979). While current thinking suggests a greater role for the extrinsic muscles in assisting MCP flexion, the intrinsic muscles are still seen as the primary MCP flexors, especially in regard to initiation of MCP flexion (Moore and Dalley, 1999; Snell, 2000).

Yet, in voluntary all-joint finger flexion movements, FDS and FDP were observed to be the primary agonists (Darling et al., 1994). In addition, MCP flexion moment arms for FDS and FDP, determined experimentally from cadaver studies, are much greater than those of the lumbricals and interossei (An et al., 1983). These

*Corresponding author. Suite 1406 Sensory Motor Performance Program, Rehabilitation Institute of Chicago, 345 E. Superior Street, Chicago, IL 606011, USA. Tel.: +1-312-238-1233; fax: +1-312-238-2208.

E-mail address: d-kamper@northwestern.edu (D.G. Kamper).

0021-9290/02/$ - see front matter
PII: S0021-9290(02)00229-4

discoveries imply that FDS and FDP participate in initiation of MCP flexion.

Two mechanisms exist by which the actions of the extrinsic flexors might be communicated to the MCP joint. First, the extrinsic flexor tendons pass through annular and cruciform pulleys attached to the finger phalanges (Bejjani and Landsmeer, 1989). These pulleys could translate force from the flexor tendons to the proximal phalanx. Second, the inherent passive resistance of the joints to rotation might allow moments created about the DIP and PIP joints to be propagated to the MCP joint.

Thus, the purpose of this research was to test whether it is biomechanically feasible for the extrinsic flexors to initiate concurrent flexion at all three finger joints, through the use of a biomechanical model of the index finger. The relative contributions of the passive joint torques and the pulley mechanisms to concurrent flexion were examined as well through the model.

2. Methods

A computer model was created to simulate FDS and FDP shortening in the index finger. Model parameters, such as segment length and diameter and passive static and dynamic resistance to joint rotation, were obtained experimentally. Model results were validated through comparison with index finger motion produced by electrical stimulation of FDS and FDP.

2.1. Model development

A two-dimensional dynamic model of the index finger was developed using the simulation software Working Model® (MSC.Software, San Mateo, CA). The index finger was used as a representative case because of its functional importance in the precision grip and its significant potential for movement independent of the other fingers (Schieber, 1991).

The finger was modeled in the mid-sagittal plane as an open-linked chain with four segments and three degrees of freedom. Revolute pin joints were used for the DIP, PIP, and MCP joints, in accordance with other models (Esteki and Mansour, 1997; Li et al., 2000; Sancho-Bru et al., 2001). The metacarpal segment was fixed in place (Fig. 1).

Model parameters such as segment length and joint diameter and passive joint characteristics were obtained from experimental measurements (Section 2.2). Finger segment volume was estimated from measured segment length and thickness. The volumes of the two proximal segments were each approximated by the frustum of a right circular cone, while the volume of the distal segment was approximated by a cylinder. In accordance with other models (Esteki and Mansour, 1997), segment

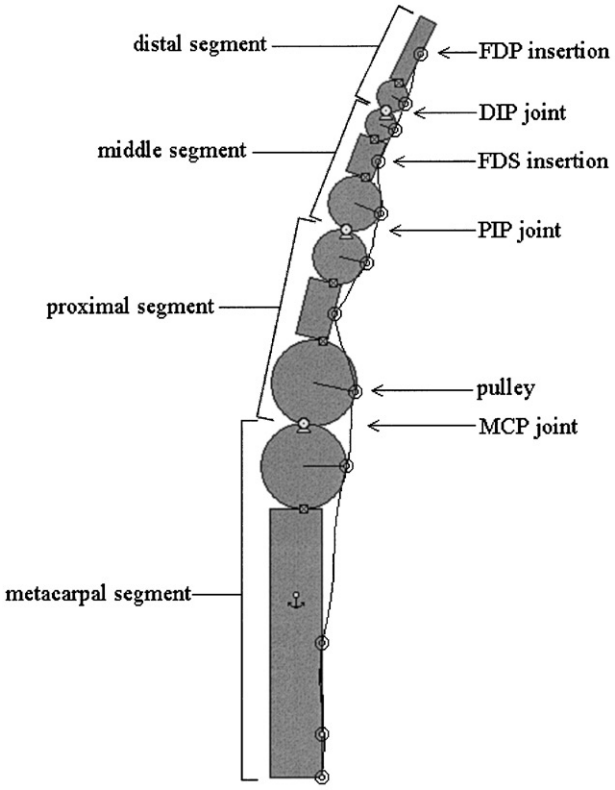

Fig. 1. Model of the index finger with three joints and four segments. Each segment is graphically represented by rigidly connected rectangle and circles. Pin joints connect each two adjacent circles. These joints include torque actuators, used to model passive joint torque. The concentric circles attached to each rectangle or circle represent pulleys through which the ropes modeling the FDP and FDS tendons run. The "FDP" rope attaches to the distal segment while the "FDS" rope attaches to the middle segment. The metacarpal segment is fixed in place, as indicated by the anchor symbol. Gravity was not included in the simulation.

mass was estimated from segment volume using a constant density (1.1 g/cm^3) (Dempster, 1955). Segment center of mass and inertia were also computed from the geometry and entered into the model.

Phalanx shape was measured in the index finger of a cadaver. Phalanx thickness for the model was obtained by scaling the measured phalanx thickness by the ratio of phalanx length measured in the human subjects to that recorded in the cadaver. Shapes corresponding to these phalanx dimensions were created within the Working Model® environment.

The finger model was actuated by two inelastic ropes that represented the FDP and FDS tendons. As with tendons, these ropes created only a tensile (not contractile) force. Rope pathway was constrained to the surface of the model phalanges by use of pulleys, simulating the annular and cruciform pulleys. The thickness of the tendons themselves (approximately 0.7 mm) was neglected.

FDS and FDP activation were simulated by shortening the lengths of the ropes in the model linearly with

time. This expression of muscle contraction in terms of muscle shortening seemed warranted due to the exquisite control of muscle length as afforded by the feedback system involving the muscle spindles in the body. Indeed, length of the extrinsic finger muscles is highly predictive of fingertip location (Biggs et al., 1999).

An FDS shortening velocity of 3.4 cm/s was simulated. This value is equivalent to a shortening of 50% of the optimal muscle fiber length over 1 s (Lieber et al., 1992), a reasonable value for lightly loaded muscle (Yamashita-Goto et al., 2001). To account for the possibly greater change in length in the FDP tendon predicated by additional DIP rotation, the FDP rate of shortening was made 20% greater than that of the FDS, as tendon length change due to DIP rotation is 20% of that produced by similar rotation of the PIP and MCP joints.

Passive joint torques were included through the use of torque actuators at each joint. The representative static and dynamic passive characteristics determined for each joint (Section 2.2) were included in the formulas to determine the torque at each joint j:

$$\tau_j = \tau_j^s - B_j\dot{\theta}_j - K_j(\theta_j)\,\Delta\theta_j, \quad (1)$$

where τ is the passive joint torque, τ^s (a function of $(\theta_j - \theta_{j+1})$) is the static passive torque, and B and K (a function of θ_j) are the damping and dynamic stiffness coefficients for joint j. The static torque was computed for the difference in joint angle between the joint of interest and the one immediately proximal to it. The value for $\Delta\theta$ was determined by subtracting the current value of the joint angle from that obtained from the model simulation 5 ms previously. This procedure was performed using the Dynamic Data Exchange between Working Model® and MATLAB® (The MathWorks, Inc., Natick, MA), which permitted sharing of data between the two programs at each simulation step.

The simulations were run until one of the joint angles approached 80° of flexion. Initial conditions were described by zero joint velocity, joint angles of DIP equal 7°, PIP equal 7°, and MCP equal 14° of flexion, and 0.3 mm of slack in the ropes. Initial joint angles were chosen based upon mean values for zero resting torque in experimental data (see Section 2.2). Joint states were updated in the software through solution of the dynamics equations using a fifth-order Runge–Kutta algorithm with a variable integration step ($\leqslant$1 ms). Angular rotations of the joints were recorded as functions of time.

2.2. Model parameters

Finger segment lengths and diameters were measured with a pair of calipers in the left index finger of six healthy adults (five males, one female, aged 21–35 years). These subjects then participated in experiments designed to determine the passive resistance to flexion/extension movement of the DIP, PIP, and MCP joints. The Institutional Review Board of Northwestern University approved the experimental protocol and the subjects gave informed consent according to the Helsinki Declaration.

The left wrist was placed in a fiberglass cast that was clamped to a table, in order to maintain neutral wrist position and orientation. The index finger was included in this cast up to the middle of the middle phalanx, thereby leaving only the DIP free to move. The finger was coupled to a servomotor (1.4 HP, PMI Motion Technologies, Radford, VA) through the use of a hose clamp, attached to the servomotor shaft through an aluminum housing. The DIP joint was aligned with the shaft of the servomotor.

Perturbations in joint angle were applied to the finger through the servomotor. Specifically, pseudo-random binary sequences (PRBS) of $\pm 2°$ in amplitude were imposed at the DIP joint at different operating points (Kearney et al., 1997). These operating points were spaced 10° apart, ranging from 10° of extension to 60° of flexion. The proportional integral derivative (PID) controller of the servomotor was tuned such that the PRBS command signals were low-pass filtered in order to reduce noise. The pass band of the angular input went beyond 20 Hz, which was considered adequate for the biological parameters of interest (Hunter and Kearney, 1982). Joint position (θ), velocity ($\dot{\theta}$), and torque (τ) were digitally sampled and then low-pass filtered at 25 Hz with a 30th-order FIR filter (Fig. 2).

The cast was then cut back to allow flexion and extension of the PIP joint, while the DIP joint was fixed

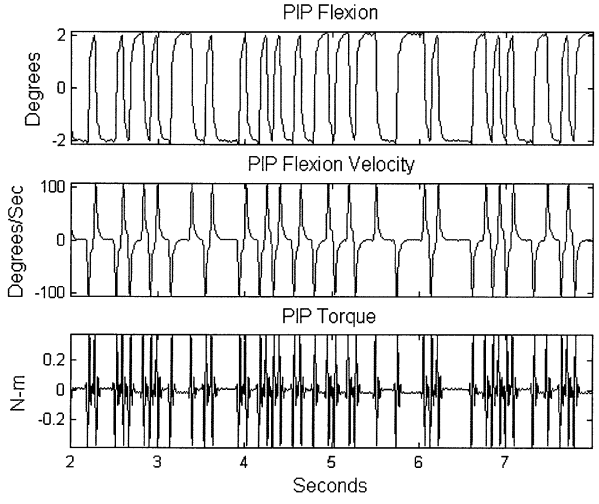

Fig. 2. Example of recorded angular position (encoder, #138647, PMI Motion Technologies), velocity (tachometer, PMI Motion Technologies), and torque (torque meter, TRT-200, Transducer Techniques, Temecula, CA), for a PRBS perturbation trial at the PIP joint. Signals were low-pass filtered at 200 Hz prior to being sampled at 500 Hz.

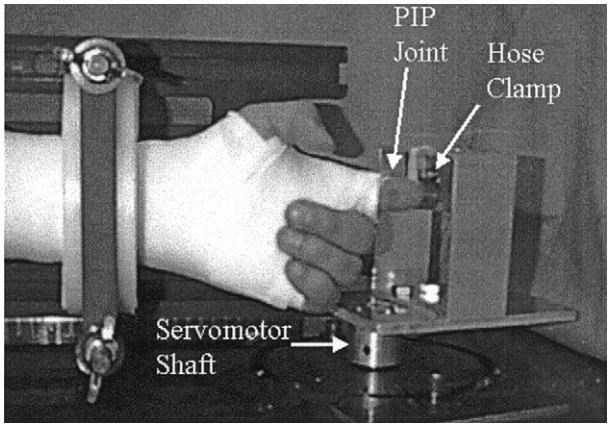

Fig. 3. Experimental configuration for determination of passive joint characteristics of the index finger. A servomotor controlled rotation about the joint of interest (the PIP joint for the situation depicted). Joints distal to the joint of interest were rigidly held in the neutral position by hose clamps.

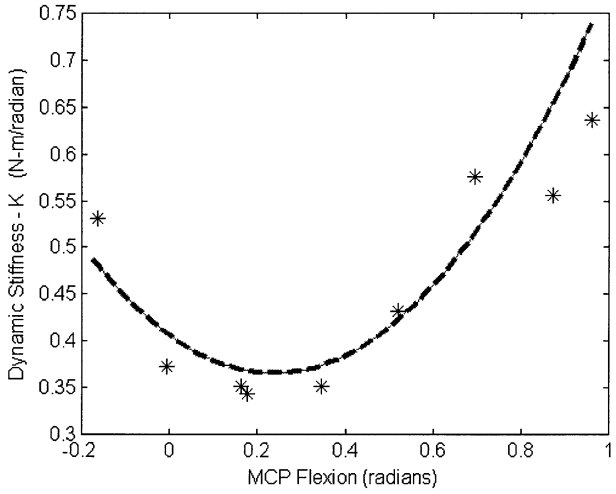

Fig. 4. Sample MCP joint stiffness as a function of MCP joint angle for one subject. Stars depict actual data points. The dashed curved depicts a parabolic stiffness function fit to the data.

in place by the hose clamp which bridged it and the MCP joint remain fixed by the cast (Fig. 3). Angle PRBS perturbations were applied to the PIP joint at each operating point.

Finally, the cast was retracted to the mid-palm to expose the MCP joint. Perturbations of the MCP joint were then performed, with both the PIP and DIP joints fixed in the neutral position by two hose clamps.

For each trial, the static and dynamic joint characteristics were determined. The static characteristics were defined by the mean torque recorded at each operating point prior to initiation of the PRBS perturbations. Across all subjects, a description of the static passive torque as a function of joint angle ($\tau^s(\theta)$) was formed by fitting a third-order polynomial to the torque-angle data using least-squares techniques in MATLAB®.

The dynamic characteristics were obtained by fitting an $I-B-K$ model with constant coefficients at each operating point such that

$$\tau = I\ddot{\theta} + B\dot{\theta} + K(\theta - \theta_0), \tag{2}$$

where I is the rotational inertia, B is the joint damping, K is the joint stiffness, and θ_0 is the operating point (Kearney et al., 1997; Hajian and Howe, 1997). The angular acceleration ($\ddot{\theta}$) was numerically computed from the angular velocity using a five-point formula. The $I-B-K$ coefficients were then fit to the data using multiple regression.

Joint damping terms exhibited no statistically significant dependence on joint angle for various regression analyses (linear, quadratic, logarithmic, exponential). Thus, representative damping terms for the model were found by computing mean values across all the subjects.

In contrast, estimations of dynamic joint stiffness did suggest a parabolic relationship between stiffness and joint angle (Fig. 4). To obtain representative values for the model, the stiffness coefficients and joint angles form the regression models for each joint (Eq. (2)) were pooled for all of the subjects. Joint stiffness was then described by fitting a second-order polynomial in joint angle to the data using least-squares techniques.

As noted previously, segment inertias for the model were computed from the mass and geometry rather than using the inertial terms resulting from the $I-B-K$ models. This was done due to the dominance of the finger clamp in its contribution to the I-coefficient. This dominance rendered determination of finger inertia from this I-coefficient questionable due to the finite precision of our transducers.

2.3. Experimental validation of model

The joint rotations obtained from the computer simulation were compared with the index finger joint rotations resulting from electrical stimulation of the FDS and FDP for the index finger in one subject (one of the authors). Intramuscular tungsten microelectrodes (50 mm/10 MΩ, Frederick Haer & Co., Inc., Bowdoinham, ME) were inserted into the muscle bellies of FDS(I) and FDP(I). Proper electrode placement was determined through electrical stimulation and visual or manual assessment of resulting finger motion or torque.

With the forearm in the neutral position, the wrist and arm were supported using the previously described clamps (Fig. 3), while the index finger was supported and separated from the other digits with a smooth plate covered in oil to minimize friction. Initial finger posture was obtained by extending the finger so that all joints were aligned in neutral and then relaxing the finger muscles, typically resulting in a posture of approximately 15° of MCP flexion and 0° of PIP and DIP

flexion. An electrical stimulator (Compex2®, Medi-Compex SA, Switzerland) provided 300 μs current pulses to the relaxed muscles either at 1 Hz twitch frequency, for verification of electrode placement, or at 30 Hz tetanus frequency for the measurement of finger motion.

Flexion/extension of the DIP, PIP, and MCP joints were measured with a video system (OPTOTRAK® 3010, Northern Digital Inc., Waterloo, Ont.). Active infrared markers were initially placed on the distal phalanx, the DIP joint, the middle phalanx, the PIP joint, the proximal phalanx, the MCP joint, and the index metacarpal bone. After the marker locations were recorded using the OPTOTRAK® system, the markers over the DIP, PIP, and MCP joints were removed so that they would not interfere with joint rotation.

Marker locations were sampled at 150 Hz while the electrical stimulation sequence was repeated several times for each trial. The locations were digitally low-pass filtered forwards and backwards at 7.5 Hz using a 30th-order finite impulse response filter. Joint angles were computed from the marker locations employing the law of cosines for the triangles formed by two adjacent phalanx markers and the joint between them, using the assumption that the joint centers of rotation did not change.

Table 1
Model parameters

Finger segment	Length (SD) (cm)	Mass (g)	Moment of inertia (g/cm^2)
Distal	2.4 (0.1)	3.8	2.0
Middle	3.1 (0.2)	6.3	5.8
Proximal	4.9 (0.3)	19.6	45.4

3. Results

Our biomechanical model showed that shortening of FDS and FDP muscles could initiate concurrent flexion at all three joints, though the inclusion of passive joint torques was necessary to achieve this. Inclusion of the pulley mechanisms in the model with segment mass and inertia (Table 1), but without passive joint torques, resulted primarily in flexion of only the PIP joint, which increased by 75° from its starting posture. The MCP and DIP joints experienced slight extension (Fig. 5).

Inclusion of the physiological static passive joint torque and the dynamic stiffness and damping (Table 2) in the computer simulation resulted in simultaneous flexion of all three joints in response to FDP and FDS shortening (Fig. 6). Rates of change of the DIP and PIP angles were greater than that of MCP.

Removal of the pulley structures connected to the proximal segment, thereby simulating avulsion of the annular pulley A2, also affected the model output. While the final joint rotation angles were quite similar (Fig. 7), the rate of change of the DIP and PIP joint angles were significantly reduced ($p<0.001$) from those obtained when all of the pulleys were intact. Removal of all of the pulleys necessitated a two-fold increase in the FDP shortening velocity to keep this rope from becoming slack during the simulation. For these conditions, net MCP flexion decreased by almost 10°.

Electrical stimulation of the FDS and FDP muscles also resulted in concurrent flexion at the DIP, PIP, and MCP joints (Fig. 8), verifying model feasibility. As in the model, total flexion was greatest at the PIP joint, with the rate of change of PIP and DIP flexion exceeding that of the MCP joint.

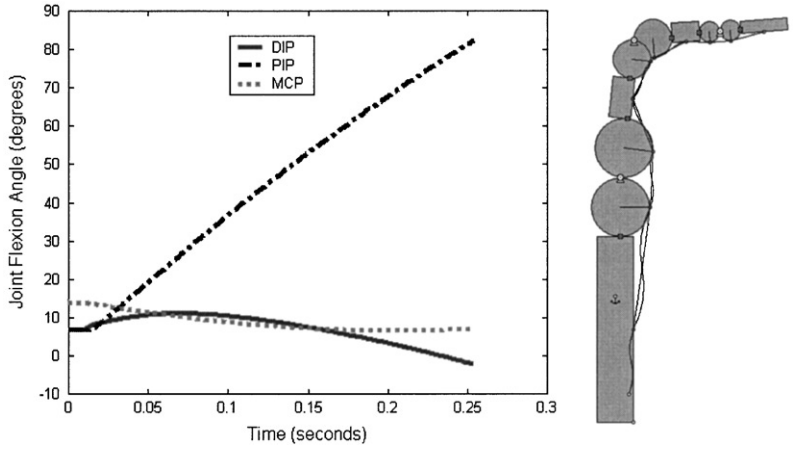

Fig. 5. Joint angles from simulation of FDS and FDP shortening with no passive joint torque. DIP: solid line; PIP: dashed-dotted line; MCP: dotted line. Accompanying model shows the animation output of the simulation at 0.25 s. Joint angles at this juncture were 2° of DIP extension, 81° of PIP flexion and 7° of MCP extension, indicating next changes of −8°, 75°, and −7° from the initial angles, respectively. The full animation is available for viewing (extrinsic_flexor_muscles_fig5.avi) (see webpage of the Journal of Biomechanics: http://www.elsevier.com/locate/jbiomech).

Table 2
Representative passive torque characteristics

Joint	Parameters		
	τ^s (N m)	K (N m/rad)	$B \times 10^2$ (SD) (N m s/rad)
DIP	$-0.103\theta^3 + 0.102\theta^2 - 0.052\theta - 0.019$	$0.38\theta^2 - 0.09\theta + 0.13$	0.81 (0.08)
PIP	$0.056\theta^3 + 0.016\theta^2 - 0.132\theta + 0.015$	$1.06\theta^2 - 0.76\theta + 0.40$	1.05 (0.13)
MCP	$-0.071\theta^3 + 0.145\theta^2 - 0.154\theta + 0.029$	$1.02\theta^2 - 0.54\theta + 0.45$	1.42 (0.23)

For the above functions, θ is given in radians with a positive value indicating flexion. The data from one subject were not included in the computation of K and B for MCP because this set exerted undue influence on the stiffness data and, thus, was not representative. Across the range of joint angles, ANOVA results and post hoc Tukey tests revealed that both the stiffness and damping coefficients were significant ($p < 0.001$) for each joint, and the $I-B-K$ model fit the data well ($R^2 > 0.96$ for each trial).

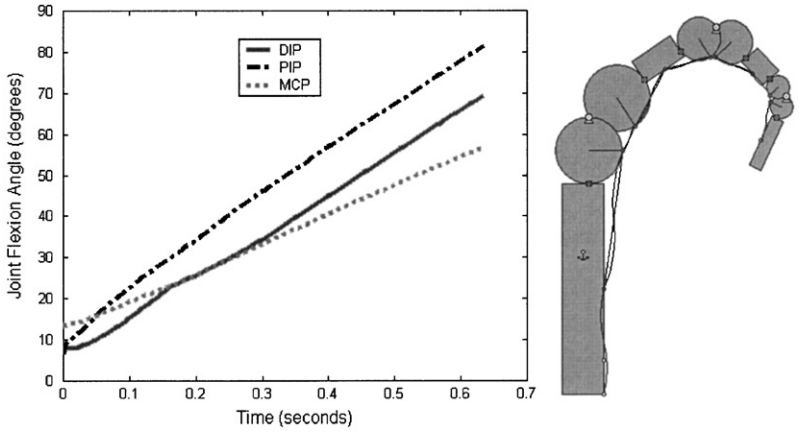

Fig. 6. Joint angles from simulation of FDS and FDP shortening with the inclusion of physiological passive joint torques. Accompanying model shows the animation output of the simulation at 0.63 s. The net angular displacements from the starting posture at this juncture were 63° for DIP, 75° for PIP, and 43° for MCP. The full animation is available for viewing (role_of_extrinsics_fig6.avi) (see webpage of the Journal of Biomechanics: http://www.elsevier.com/locate/jbiomech).

Sensitivity analyses of certain model parameters were performed to determine the effects of possible errors in measurement of these parameters. Specifically, the simulations were rerun for 50% increases in the passive torque coefficients or joint radius for each joint sequentially. The joint radius was defined by the distance from the center of rotation to the rope. The simulations were again terminated when the PIP joint reached 80°. Changes in DIP joint characteristics had negligible impact on the simulation results. The 50% increase in PIP passive torque coefficients resulted in an 11% increase in MCP flexion, while the 50% increase in PIP radius resulted in a 14% decrease in MCP flexion. At the MCP joint, increasing the torque coefficients led to a 15% decrease in MCP flexion, while increasing the radius caused a 10% increase in MCP flexion.

4. Discussion

Planning of interventions to correct impairment requires a sound knowledge of the underlying physiological infrastructure. In the case of the finger, understanding the roles of different muscles in controlling MCP flexion could help in deciding which muscles to stimulate or use for tendon transfer. The roles of the extrinsic finger muscles, especially, remain a matter of some debate.

To examine the feasibility of FDS and FDP initiating and generating MCP flexion, a biomechanical model of the index finger was created. Representative values were employed for model parameters such as finger segment length and mass. The segment lengths obtained through measurements on six subjects were similar to those reported previously (Buchner et al., 1988), with differences of not more than 4 mm. The computed masses, however, were an order of magnitude smaller than those reported elsewhere (Buchner et al., 1988), although larger than those estimated experimentally (Hajian and Howe, 1997). They do seem to be in accord, though, with anthropomorphic values expressing whole hand mass equal to 0.75% of total body mass (Seireg and Arvikar, 1989).

Phalanx thicknesses were scaled from cadaver measurements. The joint thicknesses were slightly larger than those in the literature, probably due to the larger hand size of the subjects, with the PIP thickness somewhat disproportionately larger (An et al., 1983).

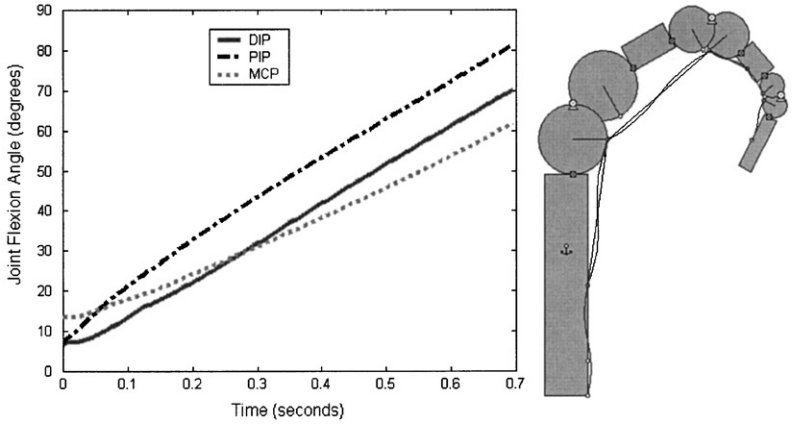

Fig. 7. Joint angles resulting from simulation of FDS and FDP shortening with the pulley mechanisms removed from the proximal segment (passive joint torque still included). Figure depicts the animation output at 0.69 s.

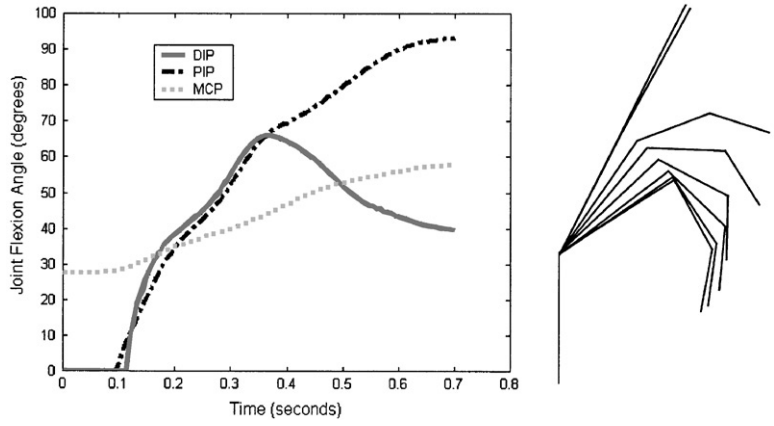

Fig. 8. Flexion at all three joints in response to electrical stimulation of FDS(I) and FDP(I) at 30 Hz. The electrode insertion site for FDP was just lateral to the flexor carpi radialis (FCR) tendon, distal to the elbow crease by approximately 60% of the distance between the elbow and wrist creases. The electrode insertion site for the FDS was just medial to the FCR tendon, distal to the FDP site (Burgar et al., 1997). To evoke finger movement, current amplitude of the tetanic pulse train was linearly increased to 2 mA over a 3 s period, held at that level for 1 s, and then ramped down to 0 mA over 3 s. Resulting rotation of all three joints is concurrent. Rate of change of DIP and PIP flexion is greater than that for MCP flexion. Kinematic representation of figure movement during electrical stimulation was obtained using MCP, PIP, and DIP joint angles from 0 to 0.7 s at 0.1 s intervals.

Representative values were also employed to describe passive static joint torque and dynamic joint stiffness and damping. The static torque values for the MCP are similar to those shown elsewhere (Esteki and Mansour, 1996) for slow MCP rotations (3°/s) from extension to flexion. Dynamic stiffness terms for the PIP and DIP joints for the extended finger are similar to those determined elsewhere, but the MCP value is more than 50% smaller (Milner and Franklin, 1998). Some of this discrepancy may be attributable to the different techniques used to obtain the stiffness, namely, PRBS perturbations of the MCP joint versus ramp displacement of the fingertip. It should be noted that due to experimental limitations joint characteristics were obtained only for displacement of the joint of interest, with the other joints being fixed.

The sensitivity analyses performed, however, suggest that the model outcome is qualitatively quite robust despite significant changes in model parameters. Shortening of the simulated FDS and FDP results in concurrent flexion of all three finger joints. Flexion is initiated simultaneously in all three joints. The electrical stimulation experiment verified these findings.

In contrast, a cadaver study utilizing static loading of the FDS tendon found that significant PIP flexion ($>50°$) occurred before the loads became sufficient to initiate MCP flexion (Delattre et al., 1983). Much of the disparity may be attributable to the difference in inputs into the system, a static force versus a dynamic change in muscle length. Another factor could be a difference in the state of the system, as might arise in passive joint characteristics in a resected cadaver specimen as compared to a live subject.

The model simulations highlighted the importance of these passive joint characteristics in promoting concurrent flexion. Without the inclusion of the passive joint torques, simulated shortening of FDP and FDS failed to produce flexion of the MCP and DIP joints. In fact, the MCP and DIP joints experienced slight extension even as the PIP joint became highly flexed.

The annular and cruciform pulleys also appear to play a role in control of finger flexion. Removal of the pulley mechanisms in the model resulted in less joint flexion for a given amount of shortening of FDS and FDP, especially for the PIP and DIP joints. This effect has also been observed in cadaver studies examining the effect of resection of the flexor pulleys on MCP rotation (Brand et al., 1975; Hamman et al., 1997). Absence of the pulleys allowed the tendons to bowstring away from the segments, thereby changing the line of action of the tendons and the effective moment arms.

Interestingly, activation of the intrinsic muscles is actually not necessary to produce MCP flexion. Of course, the intrinsics still may participate strongly in MCP flexion, as actual motor control patterns were not addressed in the study. Another study, however, suggests that the activity of the intrinsic muscles is relatively low during finger flexion, except during fast movements (Darling et al., 1994). The intrinsic may be most effective in producing extreme MCP flexion, beyond 60°.

In light of the results of this and other studies, one might propose an alternative view of the role of the intrinsic finger muscles in mediating finger flexion. The intrinsic muscles may promote MCP flexion less by exerting direct traction on the proximal phalanx than by increasing the resistance to flexion of the interphalangeal (IP) joints, so that the resultant motion produced by FDS and FDP activation is altered. Activation of the intrinsic muscles creates extension moments about the IP joints through the extensor mechanism, thereby increasing the resistance of these joints to flexion. With the increased IP resistance, activation of FDS and FDP results in greater MCP flexion. By extending this concept to other muscles and joints, it becomes conceivable that motor control of finger flexion is performed largely through active regulation of joint resistance to rotation.

Acknowledgements

This research was supported by the Richard C. and Marion Falk Research Trust and the Whittaker Foundation. The authors would like to acknowledge the work of Dr. David Lin and the late Mr. Andrew Krylow in developing the finger actuator. The authors would also like to thank Dr. Andrew Fuglevand for his advice in regard to the intramuscular stimulation.

References

An, K.N., Ueba, Y., Chao, E.Y., Cooney, W.P., Linscheid, R.L., 1983. Tendon excursion and moment arm of index finger muscles. Journal of Biomechanics 16, 419–425.

Bejjani, F.J., Landsmeer, J.M.F., 1989. Biomechanics of the hand. In: Nordin, M., Frankel, V.H. (Eds.), Basic Biomechanics of the Musculoskeletal System. Lea & Febiger, Philadelphia, PA, pp. 275–304.

Biggs, J., Horch, K., Clark, F.J., 1999. Extrinsic muscles of the hand signal fingertip location more precisely than they signal the angles of individual finger joints. Experimental Brain Research 125, 221–230.

Brand, P.W., Cranor, K.C., Ellis, J.C., 1975. Tendon and pulleys at the metacarpophalangeal joint of a finger. Journal of Bone and Joint Surgery, American Volume 57, 779–784.

Buchner, H.J., Hines, M.J., Hemami, H., 1988. A dynamic model for finger interphalangeal coordination. Journal of Biomechanics 21, 459–468.

Burgar, C.G., Valero-Cuevas, F.J., Hentz, V.R., 1997. Fine-wire electromyographic recording during force generation. American Journal of Physical Medicine and Rehabilitation 76, 494–501.

Darling, W.G., Cole, K.J., Miller, G.F., 1994. Coordination of index finger movements. Journal of Biomechanics 27, 479–491.

Delattre, J.F., Ducasse, A., Flament, J.B., Kenesi, C., 1983. The mechanical role of the digital fibrous sheath: application to reconstructive surgery of the flexor tendons. Anatomia Clinica 5, 187–197.

Dempster, W.T., 1955. Space requirements of the seated operator. WADC-TR-55-159, Aerospace Medical Research Laboratories, Wright-Patterson Air Force Base, OH (as cited in Chaffin, D.B., Andersson, G.B.J., Martin, B.J., 1999. Occupational Biomechanics. Wiley, New York).

Esteki, A., Mansour, J.M., 1996. An experimentally based nonlinear viscoelastic model joint passive moment. Journal of Biomechanics 29, 443–450.

Esteki, A., Mansour, J.M., 1997. A dynamic model of the hand with application in functional neuromuscular stimulation. Annals of Biomedical Engineering 25, 440–451.

Hajian, A.Z., Howe, R.D., 1997. Identification of the mechanical impedance at the human finger tip. Journal of Biomechanical Engineering 119, 109114.

Hamman, J., Ali, A., Phillips, C., Cunningham, B., Mass, D.P., 1997. A biomechanical study of the flexor digitorum superficialis: effects of digital pulley excision and loss of the flexor digitorum profundus. Journal of Hand Surgery, American Volume 22, 328–109114325.

Hunter, I.W., Kearney, R.E., 1982. Dynamics of human ankle stiffness variation with mean ankle torque. Journal of Biomechanics 15, 747–752.

Kearney, R.E., Stein, R.B., Parameswaran, L., 1997. Identification of intrinsic and reflex contributions to human ankle stiffness dynamics. IEEE Transactions on Biomedical Engineering 44, 493–504.

Keith, M.W., Kilgore, K.L., Peckham, P.H., Wuolloe, K.S., Creasey, G., Lemay, M., 1996. Tendon transfers and functional electrical stimulation for restoration of hand function in spinal cord injury. The Journal of Hand Surgery, American Volume 21, 89–99.

Lauer, R.T., Kilgore, K.L., Peckham, P.H., Bhadra, N., Keith, M.W., 1999. The function of the finger intrinsic muscles in response to electrical stimulation. IEEE Transactions on Rehabilitation Engineering 7, 19–26.

Li, Z.M., Zatsiorsky, V.M., Latash, M.L., 2000. Contribution of the extrinsic and intrinsic hand muscles to the moments in finger joints. Clinical Biomechanics 15, 203–211.

Lieber, R.L., Jacobson, M.D., Fazeli, B.M., Abrams, R.A., Botte, M.J., 1992. Architecture of selected muscles of the arm and forearm: anatomy and implications for tendon transfer. The Journal of Hand Surgery, American Volume 17, 787–798.

Long II, C., 1968. Intrinsic-extrinsic muscle control of the fingers. The Journal of Bone and Joint Surgery 50-A, 973–984.

Milner, T.E., Franklin, D.W., 1998. Characterization of multijoint finger stiffness: dependence on finger posture and force direction. IEEE Transactions on Biomedical Engineering 45, 1363–1375.

Moore, K.L., Dalley II, A.F., 1999. Clinically Oriented Anatomy. Lippincott Williams & Wilkins, Philadelphia, PA.

Sancho-Bru, J.L., Perez-Gonzalez, A., Vergara-Monedero, M., Giurintano, D., 2001. A 3-D dynamic model of human finger for studying free movements. Journal of Biomechanics 34, 1491–1500.

Schieber, M.H., 1991. Individuated finger movements of rhesus monkeys: a means of quantifying the independence of the digits. Journal of Neurophysiology 65, 1381–1391.

Seireg, A., Arvikar, R., 1989. Biomechanical Analysis of the Musculoskeletal Structure for Medicine and Sports. Hemisphere Publishing Corporation, New York.

Snell, R.S., 2000. Clinical Anatomy for Medical Students. Lippincott Williams & Wilkins, Philadelphia, PA.

Yamashita-Goto, K., Okuyama, R., Honda, M., Kawasaki, K., Fujita, K., Yamada, T., Nonaka, I., Ohira, Y., Yoshioka, T., 2001. Maximal and submaximal forces of slow fibers in human soleus after bed rest. Journal of Applied Physiology 91, 417–424.

Zancolli, E., 1979. Structural and Dynamic Bases of Hand Surgery, 2nd Edition.. J.B. Lippincott Company, Philadelphia, PA.